

# Topological gapless points in superconductors: from the viewpoint of symmetry

Shuntaro Sumita<sup>1,\*</sup> and Youichi Yanase<sup>2,3</sup>

<sup>1</sup>Condensed Matter Theory Laboratory, RIKEN CPR, Wako, Saitama 351-0198, Japan

<sup>2</sup>Department of Physics, Kyoto University, Kyoto 606-8502, Japan

<sup>3</sup>Institute for Molecular Science, 38 Nishigo-Naka, Myodaiji, Okazaki, Aichi 444-8585, Japan

(Dated: May 18, 2022)

Searching for topological insulators/superconductors is one central subject in recent condensed matter physics. As a theoretical aspect, various classification methods of symmetry-protected topological phases have been developed, where the topology of a gapped Hamiltonian is investigated from the viewpoint of its onsite/crystal symmetry. On the other hand, topological physics also appears in semimetals, whose gapless points can be characterized by topological invariants. Stimulated by the backgrounds, we shed light on the topology of nodal superconductors. In this paper, we review our modern topological classification theory of superconducting gap nodes in terms of symmetry. The classification method elucidates nontrivial gap structures arising from nonsymmorphic symmetry or angular momentum, which cannot be predicted by a conventional theory.

## I. INTRODUCTION

In recent condensed matter physics, topological phases of matter have attracted much attention [1–3]. So far many researchers have energetically proposed various topological materials, where the wavefunction has nontrivial topology characterized by a topological invariant. A topological invariant is well-defined for a gapped Hamiltonian, i.e., an insulator or a fully gapped superconductor. Over the past decade, theoretical studies have shown that topological numbers can be classified by symmetry and dimensionality of the system. In the early stage of the studies, classification theory based on *onsite* symmetries, namely time-reversal symmetry (TRS), particle-hole symmetry (PHS), and chiral symmetry (CS), has been developed [4–6]. The three symmetries categorize any system into ten types, which are known as Altland-Zirnbauer (AZ) classes [7, 8]. Based on the categorization, Refs. [4–6] have suggested a *topological periodic table*. One can identify, by using the table, a topological number for a (gapped) system of interest, when the AZ class and dimension of the system are determined. On the other hand, more recent studies have intensively investigated a classification problem under *crystal* symmetry as well as onsite symmetry. The first trigger of such studies was a suggestion of topological crystalline insulators by Fu [9].<sup>1</sup> After that, many researchers have challenged exhaustive classification of topological invariants based on (magnetic) point/space group symmetry, by developing various methods: band structure combinatorics [11–13], topological quantum chemistry [14–19], symmetry-based indicators [20–26], Atiyah-Hirzebruch spectral sequence [27–29], etc.

Although topology of a wavefunction can be defined only for a gapped Hamiltonian, topological invariants are useful even for *gapless* systems. Indeed, Weyl semimetals possess gapless points (Weyl points) characterized by a 2D invariant called a Chern number. In other words, when the Chern number on a certain 2D slice in the 3D Brillouin zone (BZ) is different from that on another slice, there must be Weyl point(s) between the slices. Furthermore, Refs. [30, 31] have suggested an additional topological number accompanied by the presence of rotation symmetry, which protects a Dirac point on the rotation axis in the BZ. The Dirac point is stable as long as the relevant rotation symmetry is preserved. These findings provide the following two insights. First, almost all gapless points in semimetals are characterized by (weak) topological invariants. Second, the presence or absence of the invariants determines the stability of the gapless points against fluctuations.

On the other hand, a portion of superconductors also has gapless points, called superconducting nodes. Since the momentum dependence of superconducting gap is closely related to the symmetry of superconductivity and the pairing mechanism, it is important to investigate the structure and the stability of superconducting nodes. Although previous theories have pointed out some examples of topologically protected superconducting nodes [32–42], comprehensive understanding of relationships between topology and nodes has not been obtained. Moreover, recently developed group-theoretical classification theory of superconducting gap structures have discovered unusual nodes due to nonsymmorphic crystal symmetry in multi-sublattice superconductors [42–51], or higher-spin states in multi-orbital ones [51–60]. The nontrivial nodal structures cannot be predicted by a conventional classification theory of order parameters based on point group symmetry [61–66], for the following two reasons: (1) the *order-parameter* classification is sometimes incompatible with the superconducting *gap* structure (i.e., an excitation energy in the Bogoliubov spectrum), and (2) the theory does not take into account space group symmetry and higher-spin states characteristic to superconductors with multi-degrees of freedom. Therefore, a new classification theory of superconducting nodes, which elucidates relevance with topology and resolves the above two problems, was awaited.

\* shuntaro.sumita@riken.jp

<sup>1</sup> It has been revealed that Fu's model represents a kind of fragile topological insulators [10].

Because of the above backgrounds, we have actually constructed such a modern classification theory and discovered unconventional superconducting nodes protected by crystal symmetry and topology [67–70]. In this paper, we review the method of the theory (Sec. II) and the result of the topological crystalline superconducting nodes (Sec. III). Finally, a brief summary and related topics are given in Sec. IV. The content in the paper overlaps with the Japanese review article [69] written by one of the authors and Shingo Kobayashi.

## II. METHOD

In this section, we explain modern classification method of superconducting gap nodes, using group theory and topological argument. First, for the avoidance of confusion, we introduce many terminologies and notations in Sec. II A, which are used throughout the paper. Next, in Sec. II B, we construct the topological classification theory of nodes on the high-symmetry points by using the Wigner criteria and the orthogonality test [45, 67–71].

### A. Preliminary

In this section, we define many terminologies and notations of finite-group representation theory, for preparation of the main topological classification (Sec. II B). In all the discussions below, we focus on *centrosymmetric* superconductors which possess inversion symmetry (IS)  $\mathcal{I} = \{I|\mathbf{0}\}$ .<sup>2</sup> When a superconductor of interest is paramagnetic (PM) and antiferromagnetic (AFM), it has TRS  $\mathcal{T} = \{T|\mathbf{t}_{\mathcal{T}}\}$ , while the TRS is broken for a ferromagnetic (FM) superconductor. Note that  $\mathbf{t}_{\mathcal{T}}$  represents a non-primitive translation for AFM superconductors,<sup>3</sup> while it is zero for PM superconductors. Furthermore, we restrict our target to *spin-orbit-coupled* superconductors, although the classification theory introduced below is straightforwardly applicable to spinless systems.

First, let  $G$  and  $M$  be unitary and magnetic space groups of the system of interest, respectively.  $M$  and  $G$  include a translation group  $\mathbb{T}$ , which is determined by the Bravais lattice. Due to the above assumption, the space group includes the IS  $\mathcal{I}$ . When we consider PM and AFM superconductors,  $M$  is equal to  $G + \mathcal{T}G$ , while  $M = G$  for FM superconductors. In order to construct the new classification theory resolving the problems listed in the introduction, we need to fix a specific  $\mathbf{k}$  point in the BZ. Since we are particularly interested in a classification problem of the superconducting gap structure on high-symmetry  $\mathbf{k}$  points (mirror planes and rotation axes), we focus on the operations in  $G$  ( $M$ ) leaving the  $\mathbf{k}$  points invariant modulo a reciprocal lattice vector, which generate a subgroup of  $G$  ( $M$ ). The subgroup  $\mathcal{G}^{\mathbf{k}} < G$  ( $\mathcal{M}^{\mathbf{k}} < M$ ) is called a (magnetic) little group. The factor group of the (magnetic) little group by the translation group  $\bar{\mathcal{G}}^{\mathbf{k}} = \mathcal{G}^{\mathbf{k}}/\mathbb{T}$  ( $\bar{\mathcal{M}}^{\mathbf{k}} = \mathcal{M}^{\mathbf{k}}/\mathbb{T}$ ) is called a (magnetic) little cogroup. The (magnetic) little cogroup is isomorphic to a certain (magnetic) point group. Indeed, the little cogroup satisfies

$$\bar{\mathcal{G}}^{\mathbf{k}} \cong C_s, \quad (1)$$

for mirror planes, and

$$\bar{\mathcal{G}}^{\mathbf{k}} \cong C_n \text{ or } C_{nv}, \quad (2)$$

for  $n$ -fold rotation axes ( $n = 2, 3, 4$ , and  $6$ ). Symmetry operations in the point groups  $C_s$  and  $C_n$  are explicitly represented by

$$C_s = \{E, \mathcal{M}_z\}, \quad (3)$$

$$C_n = \{E, (C_n)^1, \dots, (C_n)^{n-1}\}, \quad (4)$$

where  $E$ ,  $\mathcal{M}_z$ , and  $C_n$  are an identity operator, a mirror operator (perpendicular to the  $z$  axis), and an  $n$ -fold rotation operator, respectively. The point group  $C_{nv}$  is generated by the rotation  $C_n$  and a vertical mirror operator, whose mirror plane includes the rotation axis. In each case, the magnetic little cogroup is given by

$$\bar{\mathcal{M}}^{\mathbf{k}} \cong \begin{cases} C_s, & \text{in FM superconductors,} \\ C_s + \mathcal{T}\mathcal{I}C_s, & \text{in PM or AFM superconductors,} \end{cases} \quad (5)$$

for mirror planes, and

$$\bar{\mathcal{M}}^{\mathbf{k}} \cong \begin{cases} C_{n(v)}, & \text{in FM superconductors,} \\ C_{n(v)} + \mathcal{T}\mathcal{I}C_{n(v)}, & \text{in PM or AFM superconductors,} \end{cases} \quad (6)$$

<sup>2</sup> The notation  $g = \{p_g|\mathbf{t}_g\}$  is a conventional Seitz space group symbol with a point-group operation  $p_g$  and a translation  $\mathbf{t}_g$ .

<sup>3</sup> Even when  $\mathbf{t}_{\mathcal{T}}$  is nonzero, we treat the symmetry  $\{T|\mathbf{t}_{\mathcal{T}}\}$  as a kind of TRS, although one often calls it a magnetic translation symmetry.

for  $n$ -fold rotation axes ( $n = 2, 3, 4$ , and  $6$ ).

Next, let  $\lambda_\alpha^{\mathbf{k}}$  be a double-valued irreducible representation (IR) of the magnetic little group  $\mathcal{M}^{\mathbf{k}}$ , which represents a normal Bloch state with the crystal momentum  $\mathbf{k}$ :

$$m c_{\alpha i}^\dagger(\mathbf{k}) m^{-1} = \sum_j c_{\alpha j}^\dagger(\mathbf{k}) [\lambda_\alpha^{\mathbf{k}}(m)]_{ji}, \quad m \in \mathcal{M}^{\mathbf{k}}. \quad (7)$$

$c_{\alpha i}^\dagger(\mathbf{k})$  is a creation operator of the Bloch state with a crystal momentum  $\mathbf{k}$ .  $\alpha$  is a label of the (double-valued) IR, which corresponds to the total angular momentum of the Bloch state  $j_z = \pm 1/2, \pm 3/2, \dots$  in spin-orbit coupled systems.<sup>4</sup>  $\lambda_\alpha^{\mathbf{k}}$  is called a small corepresentation. When we consider the momentum  $\mathbf{k}$  on a twofold rotation axis in a PM superconductor, for example,  $\bar{\mathcal{M}}^{\mathbf{k}}$  is given by  $\{E, C_2, \mathcal{T}\mathcal{I}, \mathcal{T}\mathcal{M}_z\}$  [see Eq. (6)]. Equation (7) for  $m = C_2$  is then represented by

$$C_2 c_{1/2, i}^\dagger(\mathbf{k}) (C_2)^{-1} = \sum_{j=1,2} c_{1/2, j}^\dagger(\mathbf{k}) (-i\sigma_z)_{ji}, \quad (8)$$

where  $\sigma_z$  is a Pauli matrix.  $c_{1/2, i}^\dagger(\mathbf{k})$  for  $i = 1, 2$  describes the pseudo-spin-up and -down Bloch states, respectively.

Since  $\mathcal{M}^{\mathbf{k}}$  is a semi-direct product between the magnetic little cogroup  $\bar{\mathcal{M}}^{\mathbf{k}}$  and the translation group  $\mathbb{T}$ , the small corepresentation satisfies

$$\lambda_\alpha^{\mathbf{k}}(T_{\mathbf{R}}) = e^{-i\mathbf{k} \cdot \mathbf{R}}, \quad T_{\mathbf{R}} = \{E | \mathbf{R}\} \in \mathbb{T}, \quad (9)$$

where  $\mathbf{R}$  is a Bravais lattice vector. Furthermore, the algebra of  $\lambda_\alpha^{\mathbf{k}}$  obeys a factor system  $\{\omega_{\text{in}}(l_1, l_2)\} \in H^2(M, \text{U}(1)_\phi)$ ,<sup>5</sup> which arises from internal degrees of freedom (e.g. a half-integer spin of electrons)<sup>6</sup>:

$$\omega_{\text{in}}(m_1, m_2) \lambda_\alpha^{\mathbf{k}}(m_1 m_2) = \begin{cases} \lambda_\alpha^{\mathbf{k}}(m_1) \lambda_\alpha^{\mathbf{k}}(m_2), & \phi(m_1) = 1, \\ \lambda_\alpha^{\mathbf{k}}(m_1) \lambda_\alpha^{\mathbf{k}}(m_2)^*, & \phi(m_1) = -1, \end{cases} \quad (10)$$

where  $\phi: \mathcal{M} \rightarrow \mathbb{Z}_2$  is defined by

$$\phi(m) = \begin{cases} +1, & m : \text{unitary}, \\ -1, & m : \text{antiunitary}. \end{cases} \quad (11)$$

Since the projective representation  $\lambda_\alpha^{\mathbf{k}}$  complies with associativity law, the factor system satisfies the following 2-cocycle condition,

$$\omega_{\text{in}}(m_1, m_2) \omega_{\text{in}}(m_1 m_2, m_3) = \omega_{\text{in}}(m_1, m_2 m_3) \omega_{\text{in}}(m_2, m_3)^{\phi(m_1)}. \quad (12)$$

For easy treatment of the small corepresentation  $\lambda_\alpha^{\mathbf{k}}$  of the magnetic little group  $\mathcal{M}^{\mathbf{k}}$  with *infinite* number of elements, we instead consider the *finite* group (magnetic little cogroup)  $\bar{\mathcal{M}}^{\mathbf{k}}$ . A representation matrix  $\bar{\lambda}_\alpha^{\mathbf{k}}$  on  $\bar{\mathcal{M}}^{\mathbf{k}}$  corresponding to  $\lambda_\alpha^{\mathbf{k}}$  of  $\mathcal{M}^{\mathbf{k}}$  is introduced by

$$\lambda_\alpha^{\mathbf{k}}(m) = e^{-i\mathbf{k} \cdot \boldsymbol{\tau}_m} \bar{\lambda}_\alpha^{\mathbf{k}}(\bar{m}), \quad (13)$$

where  $\bar{m}$  is a representative in  $\bar{\mathcal{M}}^{\mathbf{k}}$  for  $m \in \mathcal{M}^{\mathbf{k}}$ , and

$$\boldsymbol{\tau}_m = \mathbf{t}_m - \mathbf{t}_{\bar{m}} \in \mathbb{T}, \quad (14)$$

is a Bravais lattice translation corresponding to  $m$ . Substituting (13) into (10), we obtain

$$\omega_{\text{in}}(m_1, m_2) e^{-i\mathbf{k} \cdot \boldsymbol{\nu}(m_1, m_2)} \bar{\lambda}_\alpha^{\mathbf{k}}(\overline{m_1 m_2}) = \begin{cases} \bar{\lambda}_\alpha^{\mathbf{k}}(\overline{m_1}) \bar{\lambda}_\alpha^{\mathbf{k}}(\overline{m_2}), & \phi(m_1) = 1, \\ \bar{\lambda}_\alpha^{\mathbf{k}}(\overline{m_1}) \bar{\lambda}_\alpha^{\mathbf{k}}(\overline{m_2})^*, & \phi(m_1) = -1, \end{cases} \quad (15)$$

$$\boldsymbol{\nu}(m_1, m_2) = \boldsymbol{\tau}_{m_1 m_2} - \boldsymbol{\tau}_{m_1} - p_{m_1} \boldsymbol{\tau}_{m_2} = -[\mathbf{t}_{\overline{m_1 m_2}} - \mathbf{t}_{\overline{m_1}} - p_{m_1} \mathbf{t}_{\overline{m_2}}], \quad (16)$$

<sup>4</sup> Strictly speaking,  $\alpha$  is an IR of the *finite* group  $\bar{\mathcal{M}}^{\mathbf{k}} = \mathcal{M}^{\mathbf{k}}/\mathbb{T}$ , while  $j_z$  is a basis of the *continuous* (rotation) group. Therefore there is no one-to-one correspondence between  $\alpha$  and  $j_z$ . For example, an IR  $\alpha = 1/2$  of a point group  $C_{2v}$  includes all normal Bloch states with half-integer total angular momentum  $j_z = \pm 1/2, \pm 3/2, \pm 5/2, \dots$ .

<sup>5</sup>  $H^2(M, \text{U}(1)_\phi)$  stands for the second cohomology class of the group  $M$ .

<sup>6</sup> In spin-1/2 systems, for example, a phase factor  $-1$  accompanies two-time operations of TRS ( $\mathcal{T}$ ), which means a factor system  $\omega_{\text{in}}(\mathcal{T}, \mathcal{T}) = -1$ . Supposing that  $\mathbf{k}_0$  is a time-reversal invariant momentum, therefore, the representation matrix obeys the algebra  $\lambda^{\mathbf{k}_0}(\mathcal{T}) \lambda^{\mathbf{k}_0}(\mathcal{T})^* = -\lambda^{\mathbf{k}_0}(E)$ .

TABLE I. Terminologies and notations with respect to group theory used in the paper. The first and second columns are associated with unitary groups, while the third and fourth columns are with nonunitary groups including antiunitary operators. In the table, we adopt the terminologies of Ref. [73]. Adapted with permission from Ref. [68]. Copyright © 2019 by the American Physical Society.

Terminology	Notation	Terminology	Notation	Definition
Space group	$G$	Magnetic space group	$M$	Whole crystal symmetry of the system
Little group	$\mathcal{G}^k$	Magnetic little group	$\mathcal{M}^k$	Stabilizer of $k$
Small representation	$\gamma_\alpha^k$	Small corepresentation	$\lambda_\alpha^k$	IR of (magnetic) little group
Little cogroup	$\bar{\mathcal{G}}^k$	Magnetic little cogroup	$\bar{\mathcal{M}}^k$	Factor group of (magnetic) little group by $\mathbb{T}$
N/A	$\bar{\gamma}_\alpha^k$	N/A	$\bar{\lambda}_\alpha^k$	IR of (magnetic) little cogroup

where  $p_{m_1}$  is the point-group part of the operator  $m_1$ . In Eq. (15), the nonsymmorphic part of the factor system<sup>7</sup> is described by a Bravais lattice translation  $\nu(m_1, m_2)$ , namely

$$\omega_{\text{ns}}^k(m_1, m_2) = \omega_{\text{ns}}^k(\bar{m}_1, \bar{m}_2) = e^{-ik \cdot \nu(m_1, m_2)}. \quad (17)$$

Thus, the small corepresentation  $\lambda_\alpha^k$  of the infinite group  $\mathcal{M}^k$  falls into the representation  $\bar{\lambda}_\alpha^k$  of the finite group  $\bar{\mathcal{M}}^k$ , by introducing an appropriate factor system  $\{\omega^k(m_1, m_2) = \omega_{\text{in}}(m_1, m_2)\omega_{\text{ns}}^k(m_1, m_2)\}$ .

In a similar way, a projective representation  $\bar{\gamma}_\alpha^k$  of the unitary little cogroup  $\bar{\mathcal{G}}^k$ , which corresponds to a small representation  $\gamma_\alpha^k$  of the little group  $\mathcal{G}^k$ , is naturally introduced. Supposing that the representation  $\bar{\gamma}_\alpha^k$  is concretely given, we can construct the corresponding corepresentation  $\bar{\lambda}_\alpha^k$ . For FM superconductors,  $\bar{\lambda}_\alpha^k$  is same as  $\bar{\gamma}_\alpha^k$  since  $\bar{\mathcal{M}}^k = \bar{\mathcal{G}}^k$  due to the TRS breaking. When the superconductor is PM or AFM, on the other hand, we need to consider whether the degeneracy (dimension) of the representation increases or not for the nonunitary group  $\bar{\mathcal{M}}^k = \bar{\mathcal{G}}^k + \mathfrak{I}\bar{\mathcal{G}}^k$ . Here  $\mathfrak{I} \equiv \mathcal{T}\mathcal{I}$  is a pseudo-TRS operator preserved on any  $k$  point. We can systematically solve the problem with the appropriate factor system [72, 73], by using a Wigner criterion (Herring test) [27, 73–76]<sup>8</sup>:

$$W_\alpha^{\mathfrak{I}} \equiv \frac{1}{|\bar{\mathcal{G}}^k|} \sum_{\bar{g} \in \bar{\mathcal{G}}^k} \omega^k(\mathfrak{I}\bar{g}, \mathfrak{I}\bar{g}) \chi[\bar{\gamma}_\alpha^k(\overline{(\mathfrak{I}g)^2})] = \begin{cases} 1, & \text{(a),} \\ -1, & \text{(b),} \\ 0, & \text{(c),} \end{cases} \quad (18)$$

where  $\chi$  is a character of the representation. In the (b) and (c) cases, the degeneracy (dimension) of  $\bar{\lambda}_\alpha^k$  is twice as much as that of  $\bar{\gamma}_\alpha^k$ , while  $\bar{\lambda}_\alpha^k(\bar{g})$  gives the same representation as  $\bar{\gamma}_\alpha^k(\bar{g})$  for  $\bar{g} \in \bar{\mathcal{G}}^k$  in the (a) case. For details, see Appendix A.

In the above discussion, we have introduced a lot of notations for groups and representations. For the avoidance of confusion, we summarize the notations in Table I.

## B. Topological classification of superconducting gap

In this section, we consider a topological classification method of the superconducting gap on high-symmetry points (mirror planes or rotation axes) in the BZ. Before going to the details of the theory, let us overview the general framework of the topological classification. Our theory is based on the earlier classification method of topological insulators/superconductors [4–6]. Note that, in a usual sense, a topological insulator (superconductor) is an insulator (superconductor) where the wavefunctions of electrons (Bogoliubov quasiparticles) below the bandgap have nontrivial topology. The topological invariant is defined for the (BdG) Hamiltonian on the BZ, which is represented by a  $d$ -dimensional torus. As mentioned in the introduction (Sec. I), the topological periodic table (Table II), which shows classification of the invariant based on the onsite symmetries, namely TRS ( $\mathcal{T}$ ), PHS ( $C$ ), and CS ( $\Gamma$ ), is widely spread in the present condensed matter physics [4–6]. Table II includes the tenfold AZ classes [7, 8], which are classified by four types of algebraic structure: 0,  $\mathbb{Z}$ ,  $2\mathbb{Z}$ , and  $\mathbb{Z}_2$ .

Now we apply the above classification theory of topological insulators/superconductors [4–6] to the superconducting gap classification [67, 71]. However, a bandgap cannot exist in the whole  $d$ -dimensional BZ in nodal superconductors. Therefore, we

<sup>7</sup> The factor system also satisfies the 2-cocycle condition:

$$\omega_{\text{ns}}^k(m_1, m_2) \omega_{\text{ns}}^k(m_1 m_2, m_3) = \omega_{\text{ns}}^k(m_1, m_2 m_3) \omega_{\text{ns}}^k(m_2, m_3)^{\phi(m_1)}.$$

<sup>8</sup> The Wigner criterion for the *pure* TRS tells us the presence or absence of a so-called Kramers degeneracy.

TABLE II. Correspondence between the AZ classes and the onsite symmetries: TRS ( $\mathcal{T}$ ), PHS ( $\mathcal{C}$ ) and CS ( $\Gamma$ ) [4–6]. The first–third columns represent the presence or absence of the three symmetries. The absence of symmetries is denoted by “0,” while the presence is denoted by either “+1” or “–1,” depending on whether the antiunitary operator squares to +1 or –1. The fifth–eighth columns show topological classification results of a Hamiltonian defined on a  $d$ -dimensional torus for each AZ class. Classifications in the complex classes (A, AIII) and those in the real classes (AI, . . . , CI) are respectively periodic (Bott periodicity).

$\mathcal{T}$	$\mathcal{C}$	$\Gamma$	AZ class	$d = 0$	$d = 1$	$d = 2$	$d = 3$
0	0	0	A	$\mathbb{Z}$	0	$\mathbb{Z}$	0
0	0	1	AIII	0	$\mathbb{Z}$	0	$\mathbb{Z}$
+1	0	0	AI	$\mathbb{Z}$	0	0	0
+1	+1	1	BDI	$\mathbb{Z}_2$	$\mathbb{Z}$	0	0
0	+1	0	D	$\mathbb{Z}_2$	$\mathbb{Z}_2$	$\mathbb{Z}$	0
–1	+1	1	DIII	0	$\mathbb{Z}_2$	$\mathbb{Z}_2$	$\mathbb{Z}$
–1	0	0	AII	$2\mathbb{Z}$	0	$\mathbb{Z}_2$	$\mathbb{Z}_2$
–1	–1	1	CII	0	$2\mathbb{Z}$	0	$\mathbb{Z}_2$
0	–1	0	C	0	0	$2\mathbb{Z}$	0
+1	–1	1	CI	0	0	0	$2\mathbb{Z}$

instead consider a  $p$ -dimensional sphere ( $p < d$ ) surrounding the node.  $p + 1$  is called a codimension, which shows a difference between the dimension of the BZ and that of the node. For example, when a (1D) line node exists in a 3D BZ, the codimension is  $3 - 1 = 2$ , which results in  $p = 1$ .

It is necessary to reconsider symmetry since the domain of a topological number is changed from the  $d$ -dimensional BZ to the  $p$ -dimensional sphere. On the sphere, symmetries preserving the position of the node are only allowed. In particular, the node should be fixed to a high-symmetry  $\mathbf{k}$  point (mirror plane or rotational axis) in crystalline superconductors. As mentioned in Sec. II A, a unitary little cogroup on the high-symmetry  $\mathbf{k}$  point is denoted by  $\bar{\mathcal{G}}^{\mathbf{k}}$ , and an IR of  $\bar{\mathcal{G}}^{\mathbf{k}}$  by  $\bar{\gamma}_\alpha^{\mathbf{k}}$ , which corresponds to the normal Bloch state with the momentum  $\mathbf{k}$ . Furthermore, although the TRS  $\mathcal{T}$ , the PHS  $\mathcal{C}$ , and the IS  $\mathcal{I}$  themselves do not preserve the position of the node, the combined symmetries of them are allowed on any  $\mathbf{k}$  point. Therefore, important symmetries for our classification theory are pseudo-TRS  $\bar{\mathcal{T}} \equiv \mathcal{T}\mathcal{I}$ , pseudo-PHS  $\bar{\mathcal{C}} \equiv \mathcal{C}\mathcal{I}$ , and CS  $\Gamma \equiv \mathcal{T}\mathcal{C}$ , all of which are preserved on any  $\mathbf{k}$  point. The stabilizer of the high-symmetry  $\mathbf{k}$  point is thus represented by the following group:

$$\bar{\mathcal{G}}^{\mathbf{k}} = \bar{\mathcal{G}}^{\mathbf{k}} + \bar{\mathcal{T}}\bar{\mathcal{G}}^{\mathbf{k}} + \bar{\mathcal{C}}\bar{\mathcal{G}}^{\mathbf{k}} + \Gamma\bar{\mathcal{G}}^{\mathbf{k}}. \quad (19)$$

A topological number on the high-symmetry point is defined by using the BdG Hamiltonian with the symmetry  $\bar{\mathcal{G}}^{\mathbf{k}}$ . Although the classification theory of topological insulators/superconductors [4–6] is not directly applicable to the gap classification under the symmetry  $\bar{\mathcal{G}}^{\mathbf{k}}$ , an *effective AZ* (EAZ) class is instead defined for the BdG Hamiltonian on the  $p$ -dimensional sphere. For this purpose, we execute the *Wigner criteria* [27, 73–76] for  $\bar{\mathcal{T}}$  and  $\bar{\mathcal{C}}$ ,

$$W_\alpha^{\bar{\mathcal{T}}} \equiv \frac{1}{|\bar{\mathcal{G}}^{\mathbf{k}}|} \sum_{\bar{g} \in \bar{\mathcal{G}}^{\mathbf{k}}} \omega^{\mathbf{k}}(\bar{\mathcal{T}}\bar{g}, \bar{\mathcal{T}}\bar{g}) \chi[\bar{\gamma}_\alpha^{\mathbf{k}}((\bar{\mathcal{T}}\bar{g})^2)] = \begin{cases} 1, \\ -1, \\ 0, \end{cases} \quad (18 \text{ revisited})$$

$$W_\alpha^{\bar{\mathcal{C}}} \equiv \frac{1}{|\bar{\mathcal{G}}^{\mathbf{k}}|} \sum_{\bar{g} \in \bar{\mathcal{G}}^{\mathbf{k}}} \omega^{\mathbf{k}}(\bar{\mathcal{C}}\bar{g}, \bar{\mathcal{C}}\bar{g}) \chi[\bar{\gamma}_\alpha^{\mathbf{k}}((\bar{\mathcal{C}}\bar{g})^2)] = \begin{cases} 1, \\ -1, \\ 0, \end{cases} \quad (20)$$

and the *orthogonality test* [27, 76] for  $\Gamma$ :

$$W_\alpha^\Gamma \equiv \frac{1}{|\bar{\mathcal{G}}^{\mathbf{k}}|} \sum_{\bar{g} \in \bar{\mathcal{G}}^{\mathbf{k}}} \frac{\omega^{\mathbf{k}}(\bar{g}, \Gamma)^*}{\omega^{\mathbf{k}}(\Gamma, \Gamma^{-1}\bar{g}\Gamma)^*} \chi[\bar{\gamma}_\alpha^{\mathbf{k}}(\Gamma^{-1}\bar{g}\Gamma)^*] \chi[\bar{\gamma}_\alpha^{\mathbf{k}}(\bar{g})] = \begin{cases} 1, \\ 0. \end{cases} \quad (21)$$

In the above tests, we investigate orthogonality between a basis set  $\{c_{\alpha i}^\dagger(\mathbf{k})\}$  of the normal Bloch states and another one  $\{ac_{\alpha i}^\dagger(\mathbf{k})a^{-1}\}$  transformed by the symmetry  $a$  ( $= \bar{\mathcal{T}}, \bar{\mathcal{C}},$  or  $\Gamma$ ). From Eqs. (18), (20) and (21), we obtain a set of three numbers

TABLE III. Correspondence table between the set of  $(W_\alpha^{\mathfrak{Z}}, W_\alpha^{\mathfrak{C}}, W_\alpha^\Gamma)$  and EAZ symmetry classes in centrosymmetric systems [68, 71, 77, 78]. The fifth–seventh columns show topological classification results of the IR at the  $\mathbf{k}$  point with the codimension  $p + 1$ . Note that the Bott periodicity of the real classes is reversed from that in Table II, since  $\mathfrak{Z}$  and  $\mathfrak{C}$  do not flip the momentum contrary to  $\mathcal{T}$  and  $C$ . Adapted with permission from Ref. [68]. Copyright © 2019 by the American Physical Society.

$\mathfrak{Z}(W_\alpha^{\mathfrak{Z}})$	$\mathfrak{C}(W_\alpha^{\mathfrak{C}})$	$\Gamma(W_\alpha^\Gamma)$	EAZ class	$p = 0$	$p = 1$	$p = 2$
0	0	0	A	$\mathbb{Z}$	0	$\mathbb{Z}$
0	0	1	AIII	0	$\mathbb{Z}$	0
+1	0	0	AI	$\mathbb{Z}$	$\mathbb{Z}_2$	$\mathbb{Z}_2$
+1	+1	1	BDI	$\mathbb{Z}_2$	$\mathbb{Z}_2$	0
0	+1	0	D	$\mathbb{Z}_2$	0	$2\mathbb{Z}$
-1	+1	1	DIII	0	$2\mathbb{Z}$	0
-1	0	0	AII	$2\mathbb{Z}$	0	0
-1	-1	1	CII	0	0	0
0	-1	0	C	0	0	$\mathbb{Z}$
+1	-1	1	CI	0	$\mathbb{Z}$	$\mathbb{Z}_2$

$(W_\alpha^{\mathfrak{Z}}, W_\alpha^{\mathfrak{C}}, W_\alpha^\Gamma)$ , which identifies the EAZ symmetry class of the BdG Hamiltonian on the sphere by using the knowledge of  $K$  theory [7, 8, 27]. Table III shows the correspondence between the set of  $(W_\alpha^{\mathfrak{Z}}, W_\alpha^{\mathfrak{C}}, W_\alpha^\Gamma)$  and the EAZ symmetry class.<sup>9</sup>

Furthermore, from the EAZ symmetry class, we can classify the IR at the (high-symmetry)  $\mathbf{k}$  point into an algebra  $0, \mathbb{Z}, 2\mathbb{Z}$  or  $\mathbb{Z}_2$  (Table III). In this context,  $(W_\alpha^{\mathfrak{Z}}, W_\alpha^{\mathfrak{C}}, W_\alpha^\Gamma)$  gives a symmetry-based topological classification of the Hamiltonian at each  $\mathbf{k}$  point on the plane (line). When the plane (line) intersects a normal-state Fermi surface, a node composed of the intersection line (point) on the plane (line) hosts a codimension 1, and therefore it is surrounded by a 0D sphere. In other words, superconducting gap nodes on the plane (line) are classified by a 0D topological number (see  $p = 0$  in Table III). When the classification is nontrivial ( $\mathbb{Z}, 2\mathbb{Z}$ , or  $\mathbb{Z}_2$ ), the intersection leads to a node characterized by the topological invariant. Otherwise, a gap opens at the intersection line (point).

### III. RESULTS

In Sec. II, the topological classification theory of superconducting gap nodes was introduced. Although the conventional classification of order parameters can speculate the presence or absence of nodes from the momentum dependence of basis functions [61–66], it sometimes fails to describe the correct gap structures [42–60]. On the other hand, our modern theory can exactly classify the gap structures by taking into account nonsymmorphic symmetry and higher-spin states. Indeed, we have performed comprehensive classification of gap structures on high-symmetry planes [45, 51, 67, 69, 70] and lines [51, 68–70] in the BZ. In this section, we explain various nontrivial results of topological crystalline nodes, whose topological protection is characteristic to crystalline systems, as elucidated by the studies.

#### A. Classification on high-symmetry planes: nontrivial gap structures due to nonsymmorphic symmetry

First, we introduce classification results on high-symmetry planes, where the factor system  $\omega_{\text{ns}}^{\mathbf{k}}$  accompanied by *nonsymmorphic symmetry* induces nontrivial gap structures. In the following, for example, let us consider a magnetic space group  $M = P6_3/mmc1'$ , which is one of the hexagonal and PM space groups including nonsymmorphic screw symmetry.<sup>10</sup> The PM space group represents the symmetry of odd-parity superconductor UPt<sub>3</sub>, which has been known to possess unconventional line nodes protected by nonsymmorphic symmetry [42–46, 48, 51].

<sup>9</sup>  $W_\alpha^{\mathfrak{Z}} = W_\alpha^\Gamma = 0$  in FM superconductors, since both the pseudo-TRS ( $\mathfrak{Z}$ ) and the CS ( $\Gamma$ ) are broken.

<sup>10</sup> The space group is represented by Hermann–Mauguin notation. For details, see Refs. [76, 79].

### 1. Preliminary

Since the magnetic space group  $M$  includes a mirror operator  $\mathcal{M}_z = \{M_z | \frac{\hat{z}}{2}\}$ , we focus on mirror-invariant planes  $k_z = 0$  and  $k_z = \pi$  in the BZ. The (magnetic) little groups on the planes are given by

$$\mathcal{G}^k = \mathbb{T} + \mathcal{M}_z \mathbb{T}, \quad (22)$$

$$\mathcal{M}^k = \mathcal{G}^k + \mathfrak{I} \mathcal{G}^k = \mathbb{T} + \mathcal{M}_z \mathbb{T} + \mathfrak{I} \mathbb{T} + \mathcal{M}_z \mathfrak{I} \mathbb{T}, \quad (23)$$

from which the (magnetic) little cgroups are obtained:

$$\bar{\mathcal{G}}^k = \mathcal{G}^k / \mathbb{T} = \{E, \mathcal{M}_z\}, \quad (24)$$

$$\bar{\mathcal{M}}^k = \mathcal{M}^k / \mathbb{T} = \{E, \mathcal{M}_z, \mathfrak{I}, \mathcal{M}_z \mathfrak{I}\}. \quad (25)$$

The factor system taking into account spin-orbit coupling and nonsymmorphic symmetry is as follows,

$$\omega_{\text{in}}(\mathcal{M}_z, \mathcal{M}_z) = -1, \quad \omega_{\text{in}}(\mathfrak{I}, \mathfrak{I}) = -1, \quad \omega_{\text{in}}(\mathcal{M}_z, \mathfrak{I}) = \omega_{\text{in}}(\mathfrak{I}, \mathcal{M}_z) = 1, \quad (26a)$$

$$\omega_{\text{ns}}^k(\mathcal{M}_z, \mathcal{M}_z) = 1, \quad \omega_{\text{ns}}^k(\mathfrak{I} \mathcal{M}_z, \mathfrak{I} \mathcal{M}_z) = e^{ik_z}, \quad (26b)$$

where we note that  $\omega_{\text{ns}}^k$  depends on  $k_z$  due to the existence of nonsymmorphic symmetry.

Considering  $\omega^k(\mathcal{M}_z, \mathcal{M}_z) = -1$ , we obtain projective IRs  $\tilde{\gamma}_{\pm 1/2}^k$  of the little cgroup  $\bar{\mathcal{G}}^k$ ,

$$\tilde{\gamma}_{\pm 1/2}^k(E) = 1, \quad \tilde{\gamma}_{\pm 1/2}^k(\mathcal{M}_z) = \mp i, \quad (27)$$

which corresponds to (half-integer) spin-up and spin-down states, respectively. For the spin-up one, a Wigner criterion [27, 73–76] for the pseudo-TRS [Eq. (18)] is calculated as

$$\begin{aligned} W_{+1/2}^{\mathfrak{I}} &= \frac{1}{2} \sum_{\bar{g} \in \{E, \mathcal{M}_z\}} \omega^k(\mathfrak{I} \bar{g}, \mathfrak{I} \bar{g}) \chi[\tilde{\gamma}_{+1/2}^k((\mathfrak{I} \bar{g})^2)] \\ &= \frac{1}{2} (-1 + e^{ik_z}) = \begin{cases} 0, & k_z = 0, \\ -1, & k_z = \pi. \end{cases} \end{aligned} \quad (28)$$

Therefore, a representation  $\bar{\lambda}_{+1/2}^k$  of the magnetic little cgroup  $\bar{\mathcal{M}}^k$  can be constructed as follows (see also Appendix A):

	$\bar{m}$	$E$	$\mathcal{M}_z$	$\mathfrak{I}$	$\mathcal{M}_z \mathfrak{I}$	
$\bar{\lambda}_{+1/2}^k(\bar{m})$		$\begin{pmatrix} 1 & 0 \\ 0 & 1 \end{pmatrix}$	$\begin{pmatrix} -i & 0 \\ 0 & +ie^{ik_z} \end{pmatrix}$	$\begin{pmatrix} 0 & -1 \\ 1 & 0 \end{pmatrix}$	$\begin{pmatrix} 0 & i \\ ie^{ik_z} & 0 \end{pmatrix}$	(29)

The dimension two of  $\bar{\lambda}_{+1/2}^k$  physically indicates degeneracy between the spin-up and spin-down states because of the pseudo-TRS. Even when we start from the spin-down state, therefore, a projective representation equivalent to Eq. (29) is obtained. From the above result, a small corepresentation for an element  $m \in \mathcal{M}^k$  is given by

$$\lambda_{+1/2}^k(m) = e^{-ik \cdot \mathbf{R}} \bar{\lambda}_{+1/2}^k(\bar{m}), \quad (30)$$

where  $m = \bar{m} T_{\mathbf{R}}$ ,  $\bar{m} \in \bar{\mathcal{M}}^k$ , and  $T_{\mathbf{R}} = \{E | \mathbf{R}\} \in \mathbb{T}$ .

### 2. Topological gap classification

Now let us consider the topological classification of the superconducting gap structures (Sec. II B) in this system. Before going to the main issue, we revisit a general result obtained by classification under IS; we temporarily forget the presence of the mirror symmetry in the paragraph. A set of symmetries protecting a superconducting node, namely the pseudo-TRS  $\mathfrak{I}$ , the pseudo-PHS  $\mathfrak{C}$ , and the CS  $\Gamma$ , is classified by the ten EAZ classes in Table III. The class on a general  $\mathbf{k}$  point is D or DIII for even-parity superconductivity, and C or CII for odd-parity one. In particular, let us focus on the classification of line nodes ( $p = 1$ ) in three-dimensional odd-parity superconductors, which shows no topological protection of the nodes for both class C and CII. The fact is known as Blount's theorem, claiming the absence of line nodes in (spin-orbit-coupled) odd-parity

superconductors [64, 71].<sup>11</sup> According to  $p = 0$  for the EAZ class D in Table III, furthermore, we can predict the existence of a surface node characterized by a  $\mathbb{Z}_2$  invariant in three-dimensional even-parity chiral superconductors. The node is nothing but a *Bogoliubov Fermi surface* suggested by recent theoretical studies [55, 56, 80].

From the above general results, an additional symmetry is essential for a stable line node in odd-parity superconductivity. As mentioned above, indeed, Refs. [42–46, 48, 51] have proposed a counter-example of Blount’s theorem, i.e. the existence of line nodes in the odd-parity superconductor  $\text{UPt}_3$ , by taking into account the effect of nonsymmorphic symmetry. In the following, we reproduce the counter-example from the viewpoint of the topological classification theory [45, 67]. For the purpose, let us identify the EAZ class on the mirror-invariant planes  $k_z = 0$  and  $k_z = \pi$ , supposing a Cooper pair wavefunction belonging to the  $A_u$  IR of the point group  $C_{2h}$ .<sup>12</sup> The  $A_u$  pairing symmetry results in the following factor systems:

$$\omega_{\text{in}}(\mathfrak{C}, \mathfrak{C}) = -1, \quad \omega_{\text{in}}(\mathfrak{C}, \mathcal{M}_z) = -\omega_{\text{in}}(\mathcal{M}_z, \mathfrak{C}) = 1, \quad (31a)$$

$$\omega_{\text{ns}}^k(\mathfrak{C}\mathcal{M}_z, \mathfrak{C}\mathcal{M}_z) = e^{ik_z}, \quad (31b)$$

and therefore,

$$\omega_{\text{in}}(\Gamma, \mathcal{M}_z) = -\omega_{\text{in}}(\mathcal{M}_z, \Gamma), \quad (32a)$$

$$\omega_{\text{ns}}^k(\Gamma, \mathcal{M}_z) = \omega_{\text{ns}}^k(\mathcal{M}_z, \Gamma) = 1. \quad (32b)$$

Using Eqs. (31) and (32), we apply the topological classification to the representation  $\tilde{\gamma}_{+1/2}^k$  of the normal Bloch state. The Wigner criteria for  $\mathfrak{T}$  and  $\mathfrak{C}$  [Eqs. (18) and (20)], and an orthogonality test for  $\Gamma$  [Eq. (21)] are calculated as

$$\begin{aligned} W_{+1/2}^{\mathfrak{T}} &= \begin{cases} 0, & k_z = 0, \\ -1, & k_z = \pi, \end{cases} \quad (28 \text{ revisited}) \\ W_{+1/2}^{\mathfrak{C}} &= \frac{1}{2} \left\{ \omega^k(\mathfrak{C}, \mathfrak{C}) \chi[\tilde{\gamma}_{+1/2}^k(\overline{\mathfrak{C}^2})] + \omega^k(\mathfrak{C}\mathcal{M}_z, \mathfrak{C}\mathcal{M}_z) \chi[\tilde{\gamma}_{+1/2}^k(\overline{(\mathfrak{C}\mathcal{M}_z)^2})] \right\} \\ &= \frac{1}{2} (-1 - e^{ik_z}) = \begin{cases} -1, & k_z = 0, \\ 0, & k_z = \pi, \end{cases} \quad (33) \\ W_{+1/2}^{\Gamma} &= \frac{1}{2} \left\{ \frac{\omega^k(E, \Gamma)}{\omega(\Gamma, \Gamma^{-1}E\Gamma)} \chi[\tilde{\gamma}_{+1/2}^k(E)^*] \chi[\tilde{\gamma}_{+1/2}^k(E)] \right. \\ &\quad \left. + \frac{\omega^k(\mathcal{M}_z, \Gamma)}{\omega(\Gamma, \Gamma^{-1}\mathcal{M}_z\Gamma)} \chi[\tilde{\gamma}_{+1/2}^k(\overline{\Gamma^{-1}\mathcal{M}_z\Gamma})^*] \chi[\tilde{\gamma}_{+1/2}^k(\mathcal{M}_z)] \right\} \\ &= \frac{1}{2} (1 - 1) = 0, \quad (k_z = 0, \pi). \quad (34) \end{aligned}$$

According to Table II, therefore, a classifying space of the BdG Hamiltonian on the  $k_z = 0$  ( $k_z = \pi$ ) plane is the EAZ class C (AII). Topological classification of a line node on the 2D plane ( $p = 0$ ) is 0 for the class C, and  $2\mathbb{Z}$  for the class AII. This indicates that superconducting gap structures are different on between the basal plane  $k_z = 0$  and the zone face  $k_z = \pi$ ; the  $A_u$  pair wavefunction opens its gap on  $k_z = 0$ , while a line node characterized by a  $2\mathbb{Z}$  invariant emerges on  $k_z = \pi$ . The results are entirely consistent with those of the group-theoretical arguments [42–46, 48, 51].

Now we consider the meaning of the classification results by the EAZ classes. Figure 1 schematically shows the structure of the BdG Hamiltonian with the  $A_u$  Cooper pair wavefunction. On the mirror-invariant planes ( $k_z = 0, \pi$ ), the Hamiltonian can be block-diagonalized into the two IRs  $\alpha = \pm 1/2$ , due to the presence the mirror symmetry. Let us first see the classification on the basal plane  $k_z = 0$  [Fig. 1(a)]. In the above discussion, we started from the representation matrix  $\tilde{\gamma}_{+1/2}^k$  of the IR  $\alpha = +1/2$ , which corresponds to the spin-up normal Bloch state [the lower left particle in Fig. 1(a)]. The Wigner criterion for the pseudo-TRS operator, namely  $W_{+1/2}^{\mathfrak{T}} = 0$  [Eq. (28)], indicates that a basis of an IR *nonequivalent* to  $\alpha = +1/2$  is generated by  $\mathfrak{T}$ . Therefore the lower left particle in Fig. 1(a) is mapped by  $\mathfrak{T}$  to the lower right particle, which belongs to the other IR  $\alpha = -1/2$ . Similarly, the lower left particle is mapped by  $\Gamma$  to the upper right hole, because of the orthogonality test  $W_{+1/2}^{\Gamma} = 0$  [Eq. (34)]. On the other hand, since the Wigner criterion for the pseudo-PHS operator leads to  $W_{+1/2}^{\mathfrak{C}} = -1$  [Eq. (33)],  $\mathfrak{C}$  gives a basis belonging to the *equivalent* IR, which is linearly independent of the original basis. The lower left particle in Fig. 1(a) is thus mapped by  $\mathfrak{C}$  to the upper left hole in the same IR  $\alpha = +1/2$ . For the above reason, the Hamiltonian in the  $\alpha = +1/2$  space [the red frame in Fig. 1(a)] has only the pseudo-PHS  $\mathfrak{C}$  with  $\mathfrak{C}^2 = -E$ , which indicates that the Hamiltonian block is classified into the AZ class C [7, 8].

<sup>11</sup> As shown in the later discussions, Blount’s theorem breaks down in some nonsymmorphic superconductors, since only point group symmetry is considered in his theory.

<sup>12</sup> A candidate symmetry of a superconducting order parameter in  $\text{UPt}_3$  is the IR  $E_{2u}$  of the point group  $D_{6h}$ , which corresponds to the  $A_u$  IR of the subgroup  $C_{2h}$ .

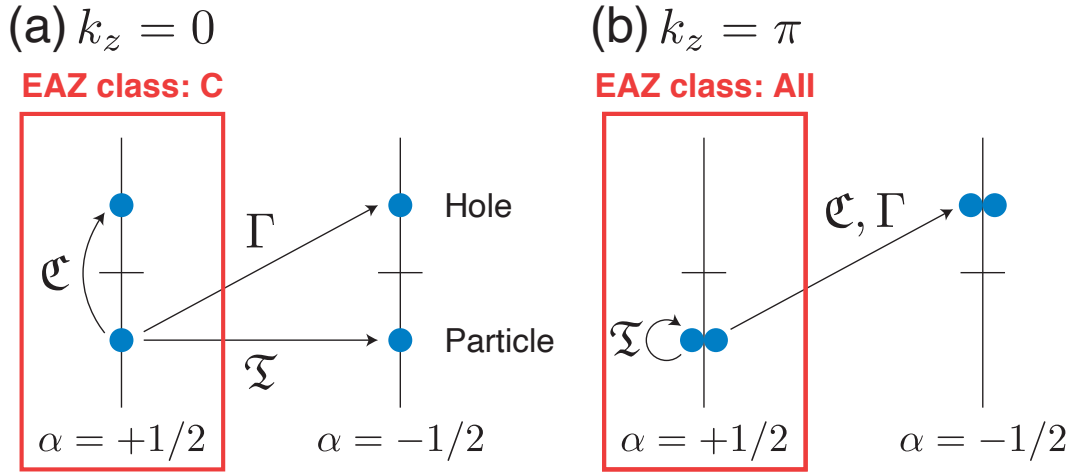


FIG. 1. Schematic pictures of the BdG Hamiltonian with an  $A_u$  pair wavefunction on (a)  $k_z = 0$  and (b)  $k_z = \pi$ . The red frames in (a) and (b) belong to EAZ classes C and AII, respectively.

TABLE IV. Group-theoretical classification of superconducting gap on high-symmetry planes. The fourth and fifth columns represent representations allowed for a gap function on the basal plane  $k_z = 0$  and the zone face  $k_z = \pi$ , respectively. The representations are decomposed into the IRs of the point group  $C_{2h}$ . A gap function should be zero, and thus, a node appears, if the corresponding IR does not exist in the reductions [81–86]; otherwise, the superconducting gap opens in general. Adapted with permission from Refs. [51, 67]. Copyright © 2018 by the American Physical Society.

Case	TRS exists?	Key ingredients	$k_z = 0$	$k_z = \pi$
(A)	No	$[\mathbf{t}_M]_z = 0$	$A_u$	$A_u$
(B)	No	$[\mathbf{t}_M]_z \neq 0$	$A_u$	$B_u$
(C)	Yes	$[\mathbf{t}_M]_z = [\mathbf{t}_T]_z = 0$	$A_g + 2A_u + B_u$	$A_g + 2A_u + B_u$
(D)	Yes	$[\mathbf{t}_M]_z = 0, [\mathbf{t}_T]_z \neq 0$	$A_g + 2A_u + B_u$	$B_g + 3A_u$
(E)	Yes	$[\mathbf{t}_M]_z \neq 0, [\mathbf{t}_T]_z = 0$	$A_g + 2A_u + B_u$	$A_g + 3B_u$
(F)	Yes	$[\mathbf{t}_M]_z \neq 0, [\mathbf{t}_T]_z \neq 0$	$A_g + 2A_u + B_u$	$B_g + A_u + 2B_u$

However, the situation is different on the zone face  $k_z = \pi$  [Fig. 1(b)]. In the case, the lower left particle in Fig. 1(b) is degenerated by  $\mathfrak{Z}$  in the equivalent IR  $\alpha = +1/2$ , because of the Wigner criterion  $W_{+1/2}^{\mathfrak{Z}} = -1$  [Eq. (28)]. On the other hand, since  $W_{+1/2}^{\mathfrak{C}} = W_{+1/2}^{\Gamma} = 0$  [Eqs. (33) and (34)], the lower left particle is mapped to the upper right holes in the nonequivalent IR  $\alpha = -1/2$ , by the pseudo-PHS  $\mathfrak{C}$  and the CS  $\Gamma$ . Therefore, the  $\alpha = +1/2$  Hamiltonian block [the red frame in Fig. 1(b)] has the pseudo-TRS  $\mathfrak{Z}$  with  $\mathfrak{Z}^2 = -E$ , and therefore belongs to the AZ class AII [7, 8].

As indicated in the above discussions, the EAZ class represents the property of a Hamiltonian block with respect to the onsite symmetries, where the block is obtained by block-diagonalizing the BdG Hamiltonian into eigenspaces (IRs) of the crystal symmetry. In general, therefore, the EAZ class of a block is different from the AZ class of the whole Hamiltonian.

We have looked in an example of a *nontrivial line node on a mirror plane stemming from nonsymmorphic symmetry* in terms of the topological classification. The classification theory is of course applicable to other various crystal symmetry and/or magnetic symmetry. Tables IV and V respectively show group-theoretical [48, 49, 51] and topological [67] classifications of gap structures in mirror- or glide-symmetric superconductors. The classification results are categorized into six types (A)-(F), where (A) and (B) represent a FM superconductor without TRS, and (C)-(F) indicate a PM or AFM one with TRS. Key ingredients of the classification are  $z$  components of  $\mathbf{t}_M$  and  $\mathbf{t}_T$ , which are translation parts of the mirror (glide) operator  $M$  and the time-reversal operator  $T$ , respectively. A nonzero  $[\mathbf{t}_M]_z$  indicates the presence of screw symmetry along the  $z$  axis in the superconductor. When  $[\mathbf{t}_T]_z$  is nonzero, on the other hand, the superconductor is in an AFM state with a  $z$ -directional propagating vector.<sup>13</sup> For example, the magnetic space group  $M = P6_3/mmc1'$  discussed above is categorized into the case (E) since it is PM and

<sup>13</sup> Remark: even when  $[\mathbf{t}_T]_z$  is zero, an AFM state with a  $x$ - or  $y$ -directional propagating vector as well as a PM state is allowed.

TABLE V. Topological classification of superconducting gap for time-reversal symmetric superconductors labeled by (C)-(F) in Table IV. The table includes classification for only zero-dimensional topological invariants. Adapted with permission from Ref. [67]. Copyright © 2018 by the American Physical Society.

Case	$A_g$		$B_g$		$A_u$		$B_u$	
	$k_z = 0$	$k_z = \pi$	$k_z = 0$	$k_z = \pi$	$k_z = 0$	$k_z = \pi$	$k_z = 0$	$k_z = \pi$
(C)	AIII, 0	AIII, 0	D, $\mathbb{Z}_2$	D, $\mathbb{Z}_2$	C, 0	C, 0	AIII, 0	AIII, 0
(D)	AIII, 0	AII, $2\mathbb{Z}$	D, $\mathbb{Z}_2$	DIII, 0	C, 0	C, 0	AIII, 0	AII, $2\mathbb{Z}$
(E)	AIII, 0	DIII, 0	D, $\mathbb{Z}_2$	AII, $2\mathbb{Z}$	C, 0	AII, $2\mathbb{Z}$	AIII, 0	C, 0
(F)	AIII, 0	D, $\mathbb{Z}_2$	D, $\mathbb{Z}_2$	AIII, 0	C, 0	AIII, 0	AIII, 0	C, 0

screw-symmetric. In general, when  $[t_M]_z$  or  $[t_T]_z$  is nonzero, namely in the cases (B), (D), (E), and (F), superconducting gap structures on the basal plane  $k_z = 0$  and the zone face  $k_z = \pi$  are different (see Table IV). That is very a consequence of nonsymmorphic symmetry.

Comparing Table IV with Table V, we find a one-to-one correspondence between the group-theoretical and topological classification theories; when the presence of a line node is predicted in the group-theoretical classification, there exists a 0D topological invariant characterizing the node. Furthermore, we have revealed that a line node in an even-parity superconductor is protected by a 1D winding number as well as the 0D invariant [67], although it is not shown in the tables. The presence of the winding number means that the node is more stable against fluctuations, and indicates the emergence of a Majorana flat band as a surface state. For further details, see Ref. [67].

### B. Classification on high-symmetry lines: nontrivial gap structures due to angular momentum

Next, let us move on to classification results on high-symmetry lines in the BZ. In this subsection, only symmorphic and PM space groups are discussed for simplicity. Nevertheless, unconventional superconducting gap structures sometimes appear on the rotation-symmetric axes because of *angular momentum of a normal Bloch state*.<sup>14</sup>

Table VI shows topological gap classification (see Sec. II B) on  $n$ -fold rotational symmetric lines in the BZ ( $n = 2, 3, 4, 6$ ) [68]. We emphasize that representations with *higher-angular-momentum states*, such as  $3/2$  and  $5/2$  spins, appear for  $n \geq 3$ , while a normal Bloch state on a twofold rotational axis always complies with spin  $1/2$ . Surprisingly, superconducting gap classification results on threefold and sixfold lines depend on the angular momentum of the normal Bloch state, although they are unique for twofold- and fourfold-symmetric cases. The *angular-momentum-dependent gap structures* are important findings in our modern classification theory [51, 68–70], since they cannot be predicted by the conventional classification theory of order parameters [61–66].

On  $C_3$ -symmetric lines, for example,  $^1E_u$  and  $^2E_u$  superconducting order parameters become gapless and gapped for the  $\alpha = +1/2$  normal Bloch state, respectively [Table VI(b1)], while both IRs are gapless for the  $\alpha = +3/2$  state [Table VI(b2)]. Indeed, we have reproduce the result in an effective model of hexagonal chiral superconductor UPt<sub>3</sub> [68]. Figures 2(b) and 2(c) show Bogoliubov quasiparticle spectra on the  $C_3$ -symmetric  $K$ - $H$  line in the BZ for  $\alpha = 3/2$  and  $\alpha = 1/2$ , respectively. Both bands generate point nodes on the line in the  $\alpha = 3/2$  state [Fig. 2(b)], whereas one band is gapless but the other is gapped for  $\alpha = 1/2$  [Fig. 2(c)]. These results are consistent with the above classification. Furthermore, there are other candidate superconductors for the unconventional angular-momentum-dependent gap structures; for details, see Refs. [51, 68–70]. One can identify superconducting gap structures in various superconductors, by using our modern classification theory.

## IV. SUMMARY

In this paper, we reviewed the modern topological classification theory of superconducting gap, and introduced various nontrivial nodal structures discovered by the theory. By considering a specific  $\mathbf{k}$  point in the BZ, our modern theory can take into account detailed properties such as nonsymmorphic symmetry and higher-spin states, which are not included in the conventional classification theory of order parameters [61–66]. Through comprehensive classification on high-symmetry planes and lines, the following important results are obtained:

<sup>14</sup> It does not mean unimportance of nonsymmorphic symmetry on the rotational axes. Indeed, Ref. [87] has found that gap structures on  $C_{2v}$ -symmetric lines sometimes become nontrivial due to glide symmetry.

TABLE VI. Topological gap classification on high-symmetry lines in the BZ. Each classification is characterized by the type of the topological number and the gap structure: (G) full gap, (P) point nodes, (L) line nodes, and (S) surface nodes (Bogoliubov Fermi surfaces). For details of point groups and their IRs, see Refs. [76, 88]. In a spontaneously TRS breaking phase, 2D IRs in  $D_{3d}$ ,  $D_{4h}$ , and  $D_{6h}$  are the same as those in  $S_6$ ,  $C_{4h}$ , and  $C_{6h}$ , respectively, since all the 2D IRs are decomposed into 1D IRs with different eigenvalues of the rotation symmetry. Therefore we do not show the 2D IRs in the tables (f), (g), and (h). Adapted with permission from Ref. [68]. Copyright © 2019 by the American Physical Society.

(a) $\bar{\mathcal{G}}^k = C_2, \alpha = \pm 1/2$			(b1) $\bar{\mathcal{G}}^k = C_3, \alpha = +[-]1/2$			(b2) $\bar{\mathcal{G}}^k = C_3, \alpha = \pm 3/2$		
IR of $C_{2h}$	EAZ	Classification	IR of $S_6$	EAZ	Classification	IR of $S_6$	EAZ	Classification
$A_g$	AIII	0 (G)	$A_g$	AIII	0 (G)	$A_g$	DIII	0 (G)
$A_u$	AIII	0 (G)	$A_u$	AIII	0 (G)	$A_u$	CII	0 (G)
$B_g$	D	$\mathbb{Z}_2$ (L)	${}^2E_g[{}^1E_g]$	D	$\mathbb{Z}_2$ (S)	${}^{1,2}E_g$	A	$\mathbb{Z}$ (S)
$B_u$	C	0 (G)	${}^1E_g[{}^2E_g]$	A	$\mathbb{Z}$ (S)	${}^{1,2}E_u$	A	$\mathbb{Z}$ (P)
			${}^2E_u[{}^1E_u]$	C	0 (G)			
			${}^1E_u[{}^2E_u]$	A	$\mathbb{Z}$ (P)			
(c) $\bar{\mathcal{G}}^k = C_4, \alpha = +[-]1/2, +[-]3/2$			(d1) $\bar{\mathcal{G}}^k = C_6, \alpha = +[-]1/2, +[-]5/2$			(d2) $\bar{\mathcal{G}}^k = C_6, \alpha = \pm 3/2$		
IR of $C_{4h}$	EAZ	Classification	IR of $C_{6h}$	EAZ	Classification	IR of $C_{6h}$	EAZ	Classification
$A_g$	AIII	0 (G)	$A_g$	AIII	0 (G)	$A_g$	AIII	0 (G)
$A_u$	AIII	0 (G)	$A_u$	AIII	0 (G)	$A_u$	AIII	0 (G)
$B_g$	A	$\mathbb{Z}$ (L)	$B_g$	A	$\mathbb{Z}$ (L)	$B_g$	D	$\mathbb{Z}_2$ (L)
$B_u$	A	$\mathbb{Z}$ (P)	$B_u$	A	$\mathbb{Z}$ (P)	$B_u$	C	0 (G)
${}^2E_g[{}^1E_g]$	D	$\mathbb{Z}_2$ (S)	${}^1E_{1g}[{}^2E_{1g}]$	D	$\mathbb{Z}_2$ (S)	${}^{1,2}E_{1g}$	A	$\mathbb{Z}$ (S)
${}^1E_g[{}^2E_g]$	A	$\mathbb{Z}$ (S)	${}^2E_{1g}[{}^1E_{1g}]$	A	$\mathbb{Z}$ (S)			
${}^2E_u[{}^1E_u]$	C	0 (G)	${}^1E_{1u}[{}^2E_{1u}]$	C	0 (G)	${}^{1,2}E_{1u}$	A	$\mathbb{Z}$ (P)
${}^1E_u[{}^2E_u]$	A	$\mathbb{Z}$ (P)	${}^2E_{1u}[{}^1E_{1u}]$	A	$\mathbb{Z}$ (P)			
			${}^{1,2}E_{2g}$	A	$\mathbb{Z}$ (S)	${}^{1,2}E_{2g}$	A	$\mathbb{Z}$ (S)
			${}^{1,2}E_{2u}$	A	$\mathbb{Z}$ (P)	${}^{1,2}E_{2u}$	A	$\mathbb{Z}$ (P)
(e) $\bar{\mathcal{G}}^k = C_{2v}, \alpha = 1/2$			(f1) $\bar{\mathcal{G}}^k = C_{3v}, \alpha = 1/2$			(f2) $\bar{\mathcal{G}}^k = C_{3v}, \alpha = 3/2$		
IR of $D_{2h}$	EAZ	Classification	IR of $D_{3d}$	EAZ	Classification	IR of $D_{3d}$	EAZ	Classification
$A_g$	CI	0 (G)	$A_{1g}$	CI	0 (G)	$A_{1g}$	AIII	0 (G)
$A_u$	CI	0 (G)	$A_{1u}$	CI	0 (G)	$A_{1u}$	C	0 (G)
$B_{1g}$	BDI	$\mathbb{Z}_2$ (L)	$A_{2g}$	BDI	$\mathbb{Z}_2$ (L)	$A_{2g}$	D	$\mathbb{Z}_2$ (L)
$B_{1u}$	BDI	$\mathbb{Z}_2$ (P)	$A_{2u}$	BDI	$\mathbb{Z}_2$ (P)	$A_{2u}$	AIII	0 (G)
$B_{2g}$	BDI	$\mathbb{Z}_2$ (L)	2D IRs	see (b1)		2D IRs	see (b2)	
$B_{2u}$	CI	0 (G)						
$B_{3g}$	BDI	$\mathbb{Z}_2$ (L)						
$B_{3u}$	CI	0 (G)						
(g) $\bar{\mathcal{G}}^k = C_{4v}, \alpha = 1/2, 3/2$			(h1) $\bar{\mathcal{G}}^k = C_{6v}, \alpha = 1/2, 5/2$			(h2) $\bar{\mathcal{G}}^k = C_{6v}, \alpha = 3/2$		
IR of $D_{4h}$	EAZ	Classification	IR of $D_{6h}$	EAZ	Classification	IR of $D_{6h}$	EAZ	Classification
$A_{1g}$	CI	0 (G)	$A_{1g}$	CI	0 (G)	$A_{1g}$	CI	0 (G)
$A_{1u}$	CI	0 (G)	$A_{1u}$	CI	0 (G)	$A_{1u}$	CI	0 (G)
$A_{2g}$	BDI	$\mathbb{Z}_2$ (L)	$A_{2g}$	BDI	$\mathbb{Z}_2$ (L)	$A_{2g}$	BDI	$\mathbb{Z}_2$ (L)
$A_{2u}$	BDI	$\mathbb{Z}_2$ (P)	$A_{2u}$	BDI	$\mathbb{Z}_2$ (P)	$A_{2u}$	BDI	$\mathbb{Z}_2$ (P)
$B_{1g}$	AI	$\mathbb{Z}$ (L)	$B_{1g}$	AI	$\mathbb{Z}$ (L)	$B_{1g}$	BDI	$\mathbb{Z}_2$ (L)
$B_{1u}$	AI	$\mathbb{Z}$ (P)	$B_{1u}$	AI	$\mathbb{Z}$ (P)	$B_{1u}$	CI	0 (G)
$B_{2g}$	AI	$\mathbb{Z}$ (L)	$B_{2g}$	AI	$\mathbb{Z}$ (L)	$B_{2g}$	BDI	$\mathbb{Z}_2$ (L)
$B_{2u}$	AI	$\mathbb{Z}$ (P)	$B_{2u}$	AI	$\mathbb{Z}$ (P)	$B_{2u}$	CI	0 (G)
2D IRs	see (c)		2D IRs	see (d1)		2D IRs	see (d2)	

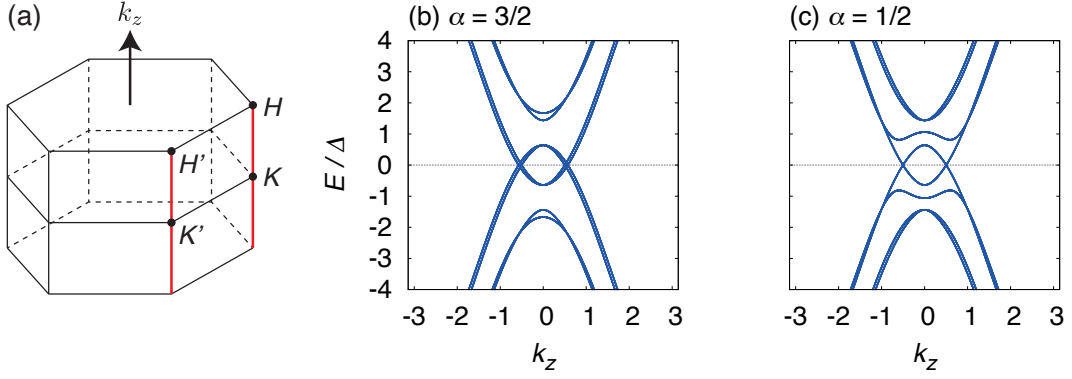


FIG. 2. (a) A threefold-rotation-invariant axis  $K$ - $H$  in a hexagonal BZ. (b, c) Quasiparticle energy spectra on the  $K$ - $H$  line in TRS broken superconductor  $\text{UPt}_3$  [68]. The normal Bloch state at the Fermi level has angular momenta  $3/2$  and  $1/2$  in (b) and (c), respectively. Adapted with permission from Refs. [51, 68]. Copyright © 2018-2019 by the American Physical Society.

- difference of gap structures on between a basal plane and a zone face attributed to *nonsymmorphic symmetry*, and
- gap structures depending on *angular momentum* of the normal Bloch state.

The classification results are determined only by symmetry, and therefore are universal and applicable to many candidate superconductors.

Finally, we mention more recent developments about the study. The first example is an uranium-based superconductor  $\text{UTe}_2$  discovered at the end of 2018 [89]. Since many previous experiments support intrinsic spin-triplet superconductivity in  $\text{UTe}_2$ , the research of this material has explosively developed. Stimulated by the backgrounds, we have discussed a detailed gap classification and the possibility of topological superconductivity, based on band structures obtained from first-principles calculations [90]. Furthermore, we have suggested unconventional gap structures protected by nonsymmorphic symmetry in  $\text{LaNiGa}_2$  [91], by using our classification method. Like the above cases, our classification method is easily applicable to various superconductors in a systematic way. In addition, more recent studies have proposed more thorough classification of topological crystalline nodes and databases of nodal superconductors [92, 93]. Based on our theory and the related studies, many other superconductors hosting unconventional nodes would be discovered.

#### ACKNOWLEDGMENT

The authors are grateful to Takuya Nomoto, Shingo Kobayashi, Ken Shiozaki, and Masatoshi Sato for fruitful discussions and collaborations on related topics. This work was supported by JST CREST Grant No. JPMJCR19T2, JSPS KAKENHI (Grants No. JP18H05227, No. JP18H01178, No. 20H05159), and SPIRITS 2020 of Kyoto University.

#### Appendix A: Wigner criterion

In this Appendix, we review the method and meaning of the Wigner criterion [27, 73–76] used in the main text. Let  $\mathfrak{G}$  be a unitary group and  $\alpha$  a  $d_\alpha$ -dimensional IR of  $\mathfrak{G}$ . We choose a certain set of basis functions  $\{\psi_1, \dots, \psi_{d_\alpha}\}$  of the IR  $\alpha$ .  $\psi_i$  transforms under the symmetry operation  $g \in \mathfrak{G}$  as

$$g\psi_i = \sum_{j=1}^{d_\alpha} \psi_j [\Delta_\alpha(g)]_{ji}, \quad (\text{A1})$$

where  $\Delta_\alpha$  is a representation matrix of the IR  $\alpha$ .

Let us consider whether the degeneracy of the IR ( $d_\alpha$ ) increases or not, by adding an antiunitary operator  $a$  to the group  $\mathfrak{G}$ . In other words, we investigate the dimension of the representation matrix for the nonunitary group  $\mathfrak{M} = \mathfrak{G} + a\mathfrak{G}$ , supposing that the information of the factor system  $\{\omega(m_1, m_2)\} \in H^2(\mathfrak{M}, U(1)_\phi)$  is given. The problem can be solved by the Wigner criterion:

$$W_\alpha^a \equiv \frac{1}{|\mathfrak{G}|} \sum_{g \in \mathfrak{G}} \omega(ag, ag) \chi[\Delta_\alpha((ag)^2)] = \begin{cases} 1, & \text{(a),} \\ -1, & \text{(b),} \\ 0, & \text{(c).} \end{cases} \quad (\text{A2})$$

For each case, indeed, the irreducible corepresentation matrix  $D_\alpha$  of  $\mathfrak{M}$ , which corresponds to  $\Delta_\alpha$  of  $\mathfrak{G}$ , is constructed as follows [27, 73, 74, 76],

$$D_\alpha(g) = \begin{cases} \Delta_\alpha(g), & \text{(a),} \\ \begin{pmatrix} \Delta_\alpha(g) & 0 \\ 0 & \Delta_\alpha(g) \end{pmatrix}, & \text{(b),} \\ \begin{pmatrix} \Delta_\alpha(g) & 0 \\ 0 & \frac{\omega(g,a)}{\omega(a,a^{-1}ga)} \Delta_\alpha(a^{-1}ga)^* \end{pmatrix}, & \text{(c),} \end{cases} \quad (\text{A3})$$

$$D_\alpha(a) = \begin{cases} U, & \text{(a),} \\ \begin{pmatrix} 0 & -U \\ U & 0 \end{pmatrix}, & \text{(b),} \\ \begin{pmatrix} 0 & \omega(a,a)\Delta_\alpha(a^2) \\ 1 & 0 \end{pmatrix}, & \text{(c),} \end{cases} \quad (\text{A4})$$

where  $U$  used in the (a) and (b) cases is a unitary matrix satisfying

$$U^\dagger \Delta_\alpha(g) U = \frac{\omega(g,a)}{\omega(a,a^{-1}ga)} \Delta_\alpha(a^{-1}ga)^*. \quad (\text{A5})$$

The meaning of each case is shown in the following.

- (a) There is no additional degeneracy due to the presence of the antiunitary operator  $a$ , because  $\{\psi_i\}$  and  $\{a\psi_i\}$  are not independent.
- (b) The presence of the operator  $a$  gives rise to additional degeneracy, because  $\{a\psi_i\}$  is linearly independent of  $\{\psi_i\}$  although they belong to the same IR  $\alpha$ .
- (c) The degeneracy is doubled by applying  $a$ , because the basis  $\{a\psi_i\}$  belongs to a representation  $\alpha'$  inequivalent to  $\alpha$ .

- 
- [1] M. Z. Hasan and C. L. Kane, *Rev. Mod. Phys.* **82**, 3045 (2010).
  - [2] X.-L. Qi and S.-C. Zhang, *Rev. Mod. Phys.* **83**, 1057 (2011).
  - [3] C.-K. Chiu, J. C. Y. Teo, A. P. Schnyder, and S. Ryu, *Rev. Mod. Phys.* **88**, 035005 (2016).
  - [4] A. P. Schnyder, S. Ryu, A. Furusaki, and A. W. W. Ludwig, *Phys. Rev. B* **78**, 195125 (2008).
  - [5] A. Kitaev, *AIP Conf. Proc.* **1134**, 22 (2009).
  - [6] S. Ryu, A. P. Schnyder, A. Furusaki, and A. W. W. Ludwig, *New J. Phys.* **12**, 065010 (2010).
  - [7] A. Altland and M. R. Zirnbauer, *Phys. Rev. B* **55**, 1142 (1997).
  - [8] M. R. Zirnbauer, *J. Math. Phys.* **37**, 4986 (1996).
  - [9] L. Fu, *Phys. Rev. Lett.* **106**, 106802 (2011).
  - [10] A. Alexandradinata, J. Höller, C. Wang, H. Cheng, and L. Lu, *Phys. Rev. B* **102**, 115117 (2020).
  - [11] R.-J. Slager, A. Mesaros, V. Juričić, and J. Zaanen, *Nat. Phys.* **9**, 98 (2012).
  - [12] J. Kruthoff, J. de Boer, J. van Wezel, C. L. Kane, and R.-J. Slager, *Phys. Rev. X* **7**, 041069 (2017).
  - [13] A. Bouhon, G. F. Lange, and R.-J. Slager, *Phys. Rev. B* **103**, 245127 (2021).
  - [14] B. Bradlyn, L. Elcoro, J. Cano, M. G. Vergniory, Z. Wang, C. Felser, M. I. Aroyo, and B. A. Bernevig, *Nature* **547**, 298 (2017).
  - [15] B. Bradlyn, L. Elcoro, M. G. Vergniory, J. Cano, Z. Wang, C. Felser, M. I. Aroyo, and B. A. Bernevig, *Phys. Rev. B* **97**, 035138 (2018).
  - [16] J. Cano, B. Bradlyn, Z. Wang, L. Elcoro, M. G. Vergniory, C. Felser, M. I. Aroyo, and B. A. Bernevig, *Phys. Rev. B* **97**, 035139 (2018).
  - [17] M. G. Vergniory, L. Elcoro, C. Felser, N. Regnault, B. A. Bernevig, and Z. Wang, *Nature* **566**, 480 (2019).
  - [18] M. G. Vergniory, B. J. Wieder, L. Elcoro, S. S. P. Parkin, C. Felser, B. A. Bernevig, and N. Regnault, All Topological Bands of All Stoichiometric Materials (2021), [arXiv:2105.09954 \[cond-mat.mtrl-sci\]](https://arxiv.org/abs/2105.09954).
  - [19] J. Cano and B. Bradlyn, *Annual Review of Condensed Matter Physics* **12**, 225 (2021).
  - [20] H. C. Po, A. Vishwanath, and H. Watanabe, *Nat. Commun.* **8**, 10.1038/s41467-017-00133-2 (2017).
  - [21] H. Watanabe, H. C. Po, and A. Vishwanath, *Sci. Adv.* **4**, eaat8685 (2018).
  - [22] E. Khalaf, H. C. Po, A. Vishwanath, and H. Watanabe, *Phys. Rev. X* **8**, 031070 (2018).
  - [23] S. Ono and H. Watanabe, *Phys. Rev. B* **98**, 115150 (2018).
  - [24] S. Ono, Y. Yanase, and H. Watanabe, *Phys. Rev. Research* **1**, 013012 (2019).
  - [25] S. Ono, H. C. Po, and H. Watanabe, *Sci. Adv.* **6**, eaaz8367 (2020).
  - [26] S. Ono, H. C. Po, and K. Shiozaki, *Phys. Rev. Research* **3**, 023086 (2021).

- [27] K. Shiozaki, M. Sato, and K. Gomi, Atiyah-Hirzebruch Spectral Sequence in Band Topology: General Formalism and Topological Invariants for 230 Space Groups (2018), [arXiv:1802.06694](https://arxiv.org/abs/1802.06694) [cond-mat.str-el].
- [28] K. Shiozaki, C. Z. Xiong, and K. Gomi, Generalized homology and Atiyah-Hirzebruch spectral sequence in crystalline symmetry protected topological phenomena (2018), [arXiv:1810.00801](https://arxiv.org/abs/1810.00801) [cond-mat.str-el].
- [29] N. Okuma, M. Sato, and K. Shiozaki, *Phys. Rev. B* **99**, 085127 (2019).
- [30] Z. Wang, Y. Sun, X.-Q. Chen, C. Franchini, G. Xu, H. Weng, X. Dai, and Z. Fang, *Phys. Rev. B* **85**, 195320 (2012).
- [31] B.-J. Yang and N. Nagaosa, *Nat. Commun.* **5**, 10.1038/ncomms5898 (2014).
- [32] T. Meng and L. Balents, *Phys. Rev. B* **86**, 054504 (2012).
- [33] J. D. Sau and S. Tewari, *Phys. Rev. B* **86**, 104509 (2012).
- [34] S. A. Yang, H. Pan, and F. Zhang, *Phys. Rev. Lett.* **113**, 046401 (2014).
- [35] G. E. Volovik, *JETP Lett.* **105**, 273 (2017).
- [36] V. Kozii, J. W. F. Venderbos, and L. Fu, *Sci. Adv.* **2**, e1601835 (2016).
- [37] J. W. F. Venderbos, V. Kozii, and L. Fu, *Phys. Rev. B* **94**, 180504 (2016).
- [38] P. Goswami and A. H. Nevidomskyy, *Phys. Rev. B* **92**, 214504 (2015).
- [39] M. H. Fischer, T. Neupert, C. Platt, A. P. Schnyder, W. Hanke, J. Goryo, R. Thomale, and M. Sigrist, *Phys. Rev. B* **89**, 020509 (2014).
- [40] A. Daido and Y. Yanase, *Phys. Rev. B* **94**, 054519 (2016).
- [41] Y. Yanase and K. Shiozaki, *Phys. Rev. B* **95**, 224514 (2017).
- [42] Y. Yanase, *Phys. Rev. B* **94**, 174502 (2016).
- [43] M. R. Norman, *Phys. Rev. B* **52**, 15093 (1995).
- [44] T. Micklitz and M. R. Norman, *Phys. Rev. B* **80**, 100506(R) (2009).
- [45] S. Kobayashi, Y. Yanase, and M. Sato, *Phys. Rev. B* **94**, 134512 (2016).
- [46] T. Nomoto and H. Ikeda, *Phys. Rev. Lett.* **117**, 217002 (2016).
- [47] T. Nomoto and H. Ikeda, *J. Phys. Soc. Jpn.* **86**, 023703 (2017).
- [48] T. Micklitz and M. R. Norman, *Phys. Rev. B* **95**, 024508 (2017).
- [49] T. Micklitz and M. R. Norman, *Phys. Rev. Lett.* **118**, 207001 (2017).
- [50] S. Sumita, T. Nomoto, and Y. Yanase, *Phys. Rev. Lett.* **119**, 027001 (2017).
- [51] S. Sumita and Y. Yanase, *Phys. Rev. B* **97**, 134512 (2018).
- [52] T. Nomoto, K. Hattori, and H. Ikeda, *Phys. Rev. B* **94**, 174513 (2016).
- [53] Y. Wan and Q.-H. Wang, *Europhys. Lett.* **85**, 57007 (2009).
- [54] P. M. R. Brydon, L. Wang, M. Weinert, and D. F. Agterberg, *Phys. Rev. Lett.* **116**, 177001 (2016).
- [55] D. F. Agterberg, P. M. R. Brydon, and C. Timm, *Phys. Rev. Lett.* **118**, 127001 (2017).
- [56] C. Timm, A. P. Schnyder, D. F. Agterberg, and P. M. R. Brydon, *Phys. Rev. B* **96**, 094526 (2017).
- [57] L. Savary, J. Ruhman, J. W. F. Venderbos, L. Fu, and P. A. Lee, *Phys. Rev. B* **96**, 214514 (2017).
- [58] I. Boettcher and I. F. Herbut, *Phys. Rev. Lett.* **120**, 057002 (2018).
- [59] H. Kim, K. Wang, Y. Nakajima, R. Hu, S. Ziemak, P. Syers, L. Wang, H. Hodovanets, J. D. Denlinger, P. M. R. Brydon, D. F. Agterberg, M. A. Tanatar, R. Prozorov, and J. Paglione, *Sci. Adv.* **4**, eaao4513 (2018).
- [60] J. W. F. Venderbos, L. Savary, J. Ruhman, P. A. Lee, and L. Fu, *Phys. Rev. X* **8**, 011029 (2018).
- [61] G. E. Volovik and L. P. Gor'kov, *Pis'ma Zh. Eksp. Teor. Fiz.* **39**, 550 (1984).
- [62] G. E. Volovik and L. P. Gor'kov, *Zh. Eksp. Teor. Fiz.* **88**, 1412 (1985).
- [63] P. W. Anderson, *Phys. Rev. B* **30**, 4000 (1984).
- [64] E. I. Blount, *Phys. Rev. B* **32**, 2935 (1985).
- [65] K. Ueda and T. M. Rice, *Phys. Rev. B* **31**, 7114 (1985).
- [66] M. Sigrist and K. Ueda, *Rev. Mod. Phys.* **63**, 239 (1991).
- [67] S. Kobayashi, S. Sumita, Y. Yanase, and M. Sato, *Phys. Rev. B* **97**, 180504(R) (2018).
- [68] S. Sumita, T. Nomoto, K. Shiozaki, and Y. Yanase, *Phys. Rev. B* **99**, 134513 (2019).
- [69] S. Sumita and S. Kobayashi, *Kotai Butsuri* **55**, 463 (2020).
- [70] S. Sumita, *Modern Classification Theory of Superconducting Gap Nodes* (Springer, Singapore, 2021).
- [71] S. Kobayashi, K. Shiozaki, Y. Tanaka, and M. Sato, *Phys. Rev. B* **90**, 024516 (2014).
- [72] C. J. Bradley and B. L. Davies, *Rev. Mod. Phys.* **40**, 359 (1968).
- [73] C. J. Bradley and A. P. Cracknell, *The Mathematical Theory of Symmetry in Solids* (Oxford University Press, Oxford, 1972).
- [74] E. P. Wigner, *Group Theory and its Application to the Quantum Mechanics of Atomic Spectra* (Academic Press, New York, 1959).
- [75] C. Herring, *Phys. Rev.* **52**, 361 (1937).
- [76] T. Inui, Y. Tanabe, and Y. Onodera, *Group theory and its applications in physics*, Springer Series in Solid-State Sciences, Vol. 78 (Springer, Berlin, 1990).
- [77] Y. X. Zhao, A. P. Schnyder, and Z. D. Wang, *Phys. Rev. Lett.* **116**, 156402 (2016).
- [78] T. Bzdušek and M. Sigrist, *Phys. Rev. B* **96**, 155105 (2017).
- [79] M. I. Aroyo, ed., *International Tables for Crystallography*, 6th ed., Vol. A: Space-group symmetry (Wiley, New York, 2016).
- [80] P. M. R. Brydon, D. F. Agterberg, H. Menke, and C. Timm, *Phys. Rev. B* **98**, 224509 (2018).
- [81] Y. Izyumov, V. Laptev, and V. Syromyatnikov, *Int. J. Mod. Phys. B* **3**, 1377 (1989).
- [82] V. G. Yarzhemsky and E. N. Murav'ev, *J. Phys.: Condens. Matter* **4**, 3525 (1992).
- [83] V. G. Yarzhemsky, *Phys. Status Solidi B* **209**, 101 (1998).
- [84] V. G. Yarzhemsky, *Int. J. Quant. Chem.* **80**, 133 (2000).
- [85] V. G. Yarzhemsky, *AIP Conf. Proc.* **678**, 343 (2003).
- [86] V. G. Yarzhemsky, *J. Opt. Adv. Mater.* **10**, 1759 (2008).

- [87] T. Yoshida, A. Daido, N. Kawakami, and Y. Yanase, *Phys. Rev. B* **99**, 235105 (2019).
- [88] Bilbao Crystallographic Server, Point Group Tables, <http://www.cryst.ehu.es/rep/point>.
- [89] S. Ran, C. Eckberg, Q.-P. Ding, Y. Furukawa, T. Metz, S. R. Saha, I.-L. Liu, M. Zic, H. Kim, J. Paglione, and N. P. Butch, *Science* **365**, 684 (2019).
- [90] J. Ishizuka, S. Sumita, A. Daido, and Y. Yanase, *Phys. Rev. Lett.* **123**, 217001 (2019).
- [91] J. R. Badger, Y. Quan, M. C. Staab, S. Sumita, A. Rossi, K. P. Devlin, K. Neubauer, D. S. Shulman, J. C. Fettinger, P. Klavins, S. M. Kauzlarich, D. Aoki, I. M. Vishik, W. E. Pickett, and V. Taufour (2021), in preparation.
- [92] S. Ono and K. Shiozaki, Symmetry-based approach to nodal structures: Unification of compatibility relations and point-node classifications (2021), [arXiv:2102.07676](https://arxiv.org/abs/2102.07676) [cond-mat.supr-con].
- [93] F. Tang, S. Ono, X. Wan, and H. Watanabe, High-throughput Investigations of Topological and Nodal Superconductors (2021), [arXiv:2106.11985](https://arxiv.org/abs/2106.11985) [cond-mat.supr-con].